

An ab-initio theoretical investigation of the soft-magnetic properties of permalloys

S.Ostanin ^{a,1} J.B.Staunton ^{a,*} S.S.A.Razee ^b B.Ginatempo ^c
Ezio Bruno ^c

^a*Department of Physics, University of Warwick, Coventry CV4 7AL, U.K.*

^b*Department of Physics, University of Kuwait, SAFAT 13060, Kuwait*

^c*Dipartimento di Fisica and Unità INFM, Università di Messina, Salita Sperone
31, I-98166 Messina, Italy*

Abstract

We study Ni₈₀Fe₂₀-based permalloys with the relativistic spin-polarized Korringa-Kohn-Rostoker electronic structure method. Treating the compositional disorder with the coherent potential approximation, we investigate how the magnetocrystalline anisotropy, K , and magnetostriction, λ , of Ni-rich Ni-Fe alloys vary with the addition of small amounts of non-magnetic transition metals, Cu and Mo. From our calculations we follow the trends in K and λ and find the compositions of Ni-Fe-Cu and Ni-Fe-Mo where both are near zero. These high permeability compositions of Ni-Fe-Cu and Ni-Fe-Mo match well with those discovered experimentally. We monitor the connection of the magnetic anisotropy with the number of minority spin electrons N_{\downarrow} . By raising N_{\downarrow} via artificially increasing the band-filling of Ni₈₀Fe₂₀, we are able to reproduce the key features that underpin the magnetic softening we find in the ternary alloys. The effect of band-filling on the dependence of magnetocrystalline anisotropy on atomic short-range order in Ni₈₀Fe₂₀ is also studied. Our calculations, based on a static concentration wave theory, indicate that the susceptibility of the high permeability of the Ni-Fe-Cu and Ni-Fe-Mo alloys to their annealing conditions is also strongly dependent on the alloys' compositions. An ideal soft magnet appears from these calculations.

Key words: Theoretical magnetism,, soft magnets, permalloys,, ab-initio electronic structure calculations

PACS: 75.30Gw, 71.20Be, 75.50Bb

* Corresponding author.

Email address: j.b.staunton@warwick.ac.uk (J.B.Staunton).

¹ Present address: Department of Earth Sciences, University College London, Gower Street, London WC1E 6BT

1 Introduction

For a magnet to be soft, weak fields must be able to change the overall magnetisation readily. Such high permeability comes about because the energies of the domain walls are low so that the magnetic anisotropy constants, K , are also very small. The internal stresses caused by the changes of magnetisation must also be minimal making the magnetostriction coefficients, λ , as small as possible.[1] Roughly the magnetic permeability is proportional to M_s^2/K_{eff} , where M_s is the saturation magnetisation and K_{eff} is a measure of magnetic anisotropy and magnetostriction, $K_{eff} = K_{eff}(K, \lambda)$.

Some of the magnetically softest ferromagnetic materials are based on the $\text{Ni}_{80}\text{Fe}_{20}$ permalloy and their high permeability finds them numerous applications in, for example, magnetic recording heads, spin valve devices and electrical power generation. In binary $\text{Ni}_{1-c}\text{Fe}_c$ alloys, K and λ both vary with concentration c and in the vicinity of $c = 0.2$ pass through zero at slightly different compositions and so the addition of a third or fourth component is required to achieve 'the focus of zero'. [2] General guidelines for achieving near zero anisotropy and magnetostriction in ternary and quaternary $\text{Ni}_{80}\text{Fe}_{20}$ -based permalloys are now well established thanks to experimental work on hundreds of samples. [3,4,5]

Recently we have carried out a theoretical investigation for a prototypical soft magnetic metal, body-centered cubic (bcc) iron [6], and have examined how its K and λ would vary if its lattice spacing (volume) and number of valence electrons (band-filling) could be altered. We have found that on reducing the band-filling and increasing the volume, iron's magnetic properties soften considerably. This situation can be realised in practice by doping bcc Fe with vanadium. We then tested our model by an explicit study of iron-rich Fe-V alloys and found the optimal composition for the smallest K and λ . In particular, we found that $\text{Fe}_{0.9}\text{V}_{0.1}$ is a high permeability material. Good agreement with experimental values for the magnetocrystalline anisotropy energy (MAE) and magnetostriction of both Fe and FeV was found.

In this paper, we start instead from a binary component 'parent' soft magnet, $\text{Ni}_{1-c}\text{Fe}_c$ with $c \approx 0.2$ and see if a similar, ab-initio approach can explain how the addition of small amounts of non-magnetic impurities, Cu and Mo, produce the magnetically softest permalloys. Our approach is based on the spin-polarized relativistic Korringa-Kohn-Rostoker (SPR-KKR) density functional theoretical (DFT) method, within the coherent-potential approximation (CPA) [7,8] for randomly disordered alloys. We explore the variation of the two main factors, K and λ , in $\text{Ni}_{1-c}\text{Fe}_{c-x}\text{Cu}(\text{Mo})_x$ with concentrations c and x and find the values which bring both quantities to optimally low values to promote high permeability. James *et al.* [9] have also recently carried out studies of the

magnetostriction and magnetic anisotropy of 3d transition metal alloys from a ‘first principles’ electronic structure framework. From their calculations, they propose that the trends are linked to the number of occupied minority spin d-states. We see if such a link is evident from our calculations here on binary and ternary permalloys.

The magnetic anisotropy constants K of Ni-rich permalloys depend also on the existence of the long- and short-range order. There is a $L1_2(\text{Cu}_3\text{Au})$ -ordered Ni_3Fe phase below 600°C . The high permeability values of technically important 80 % Ni permalloys are achieved by specified annealing in the ordered range Ni_3Fe . Here, the manufacturing processes and final heat treatment of permalloys are very important role for the alloys’ microstructures and also their final magnetic properties (coercivity, hysteresis loop shape etc.). Consequently, we also present here a study of the effect of compositional order on the high permeability $\text{Ni}_{80}\text{Fe}_{20}$ alloy and how this may be expected to vary when a non-magnetic transition metal dopant is added. This builds on our earlier work in which we described why directional chemical order and significant uniaxial magnetic anisotropy is induced in permalloy when it is annealed in a magnetic field. [8]

In the next section we briefly summarise our approach for calculating the MAE of metals and alloys, using the SPR-KKR method. We then show how the magnetostriction can also be found. In the following section we use the SPR-KKR method to study $\text{Ni}_{1-c}\text{Fe}_c$, ($c \approx 0.2$) and related Ni-Fe-Cu and Ni-Fe-Mo ternary alloys focussing on the region where high permeability appears. We discuss these results in terms of band-filling (number of valence electrons per atom) and the number of minority spin electrons plus features from the electronic densities of states. We interpret a key feature of our results by a further investigation of $\text{Ni}_{80}\text{Fe}_{20}$ in which the effect of doping with a non-magnetic impurity is modelled simply. The next section outlines the theoretical framework for compositional order in alloys and the theory for MAE in context of its dependence upon atomic short-range compositional order. The penultimate section presents our calculation of the dependence of MAE with compositional order in $\text{Ni}_{0.8}\text{Fe}_{0.2}$ and also analyses how much this varies with hypothetical band-filling. We deduce that the sensitivity of the high permeabilities of the $\text{Ni}_{0.8}\text{Fe}_{0.2-x}\text{Cu}_x$ to annealing conditions is itself dependent on the precise composition. The final section summarises and concludes.

2 Magnetic Anisotropy of Metals and Alloys.

Magnetic anisotropy of a material derives largely from spin-orbit coupling of the electronic structure. Both the origin of this effect, as well as the magnetostatic effects which determine domain structure, can be found from the

relativistic generalisation of spin density functional theory. [10] From the formal starting point of the quantum electrodynamics of electrons interacting with an electromagnetic field, a system's ground state energy is the minimum of a functional of the charge and current densities. This minimisation is achieved, in principle, by the self-consistent solution of a set of Kohn-Sham Dirac equations for independent electrons moving in fields set by the charge and current densities. Once approximations for exchange-correlation and the Gordon decomposition of the current into orbital and spin pieces are made, the spin-orbit coupling effects upon the electronic structure can be represented and the magnetic anisotropy described. (The magnetostatic shape anisotropy is also described from within the same theoretical framework [10] but not considered for the cubic materials of this paper.)

Most theoretical investigations of MAE and calculations of the anisotropy constants K place their emphasis on spin-orbit coupling effects using either perturbation theory or a fully relativistic theory, e.g. [9,7]. Typically the total energy, or the single-electron contribution to it (if the force theorem is used [11]), is calculated for two magnetisation directions, \mathbf{e}_1 and \mathbf{e}_2 separately, i.e. $F_{\mathbf{e}_1}$, $F_{\mathbf{e}_2}$, and then the MAE, ΔF , is obtained from the difference between them i.e.

$$\Delta F(\mathbf{e}_1, \mathbf{e}_2) = \int_{E_F^1}^{E_F^2} \varepsilon n_{\mathbf{e}_1}(\varepsilon) d\varepsilon - \int_{E_F^1}^{E_F^2} \varepsilon n_{\mathbf{e}_2}(\varepsilon) d\varepsilon \quad (1)$$

where E_F^1 , E_F^2 are the Fermi energies when the system is magnetised along the directions \mathbf{e}_1 and \mathbf{e}_2 respectively and $n_{\mathbf{e}_{1(2)}}$ the electronic density of states. However, the MAE is a small part of the total energy of the system, in many cases of the order of μeV and it is numerically more precise to calculate the difference directly [7]. We follow this rationale here for the study of soft magnetism and calculate the MAE from

$$\Delta F = - \int_{E_{F_1}}^{E_{F_2}} [N(\varepsilon; \mathbf{e}_1) - N(\varepsilon; \mathbf{e}_2)] d\varepsilon - \frac{1}{2} n(E_{F_2}; \mathbf{e}_2) (E_{F_1} - E_{F_2})^2 + \mathcal{O}(E_{F_1} - E_{F_2})^3 \quad (2)$$

where $N(\varepsilon; \mathbf{e})$ represents the density of states of a system magnetised along \mathbf{e} integrated up to energy ε . In most cases, the second term is very small in comparison with the first. For a binary component disordered alloy, $A_{1-c}B_c$, the MAE can be written using the Lloyd formula [12] for the integrated density of states in Eq. (3) to get

$$\Delta F = -\frac{1}{\pi} \Im \int_{E_{F_1}}^{E_{F_2}} d\varepsilon \left[\frac{1}{\Omega_{BZ}} \int d\mathbf{k} \ln \|I + [t_c^{-1}(\mathbf{e}_2) - t_c^{-1}(\mathbf{e}_1)] \tau_c(\mathbf{k}; \mathbf{e}_1)\| \right]$$

$$\begin{aligned}
& + (1 - c)\{\ln \|D_A(\mathbf{e}_1)\| - \ln \|D_A(\mathbf{e}_2)\|\} + c\{\ln \|D_B(\mathbf{e}_1)\| - \ln \|D_B(\mathbf{e}_2)\|\} \Big] \\
& - \frac{1}{2}n(E_{F_2}; \mathbf{e}_2)(E_{F_1} - E_{F_2})^2 + \mathcal{O}(E_{F_1} - E_{F_2})^3
\end{aligned} \tag{3}$$

In Eq. (3), $t_c(\mathbf{e}_1)$ and $t_c(\mathbf{e}_2)$ are the SPR-KKR-CPA t-matrices for magnetisation along \mathbf{e}_1 and \mathbf{e}_2 directions respectively and $\tau_c(\mathbf{k}; \mathbf{e}_1)$ is the scattering path-operator

$$\tau_c(\mathbf{k}; \mathbf{e}_1) = [t_c^{-1}(\mathbf{e}_1) - g(\mathbf{k})]^{-1} \tag{4}$$

and τ_c^{00} is its integral over the Brillouin zone. $D_A(\mathbf{e}_1)$ is found from

$$D_A(\mathbf{e}_1) = [I - \tau_c^{00}(\mathbf{e}_1)\{t_c^{-1}(\mathbf{e}_1) - t_A^{-1}(\mathbf{e}_1)\}]^{-1} \tag{5}$$

with similar expressions for $D_A(\mathbf{e}_2)$, $D_B(\mathbf{e}_1)$, and $D_B(\mathbf{e}_2)$. Note that $t_A(\mathbf{e}_2)$ and $t_B(\mathbf{e}_2)$, the single site t-matrices for A and B atoms respectively spin-polarised along \mathbf{e}_2 , can be obtained directly from $t_A(\mathbf{e}_1)$ and $t_B(\mathbf{e}_1)$ respectively by simple rotational transformations.[7] The numerical accuracy of our SPR-KKR-CPA calculations is to within 0.1 μeV (or 10^4 erg/cm^3) and thus the scheme is suited for studies of magnetically soft alloys. Full details of the method can be found elsewhere. [7,8,13]

3 Magnetostriction

The magnetostriction constant λ_{001} represents the relative change of length ($\delta l/l$) measured along [001] when an external magnetic field is applied along to the direction of observation. For a cubic system λ_{001} appears in the expression [14]

$$B_1 = -\frac{3}{2}\lambda_{001}(C_{11} - C_{12}), \tag{6}$$

where, B_1 is the rate of change of the MAE, $\Delta F((001), (100))$, with tetragonal strain, t , along [001], at $t = 0$. C_{11} and C_{12} are the cubic elastic constants which are related to the tetragonal shear (C') modulus: $C' = (C_{11} - C_{12})/2$. λ_{001} of Fe, calculated from this expression using a full-potential DFT method, has a large value in comparison with experiment.[15,16] Freeman and co-workers have estimated $C_{11} - C_{12}$ from a fit of their calculated total energies to simple quadratic functions of the tetragonal distortion t and calculate B_1 from the gradient of the energy difference $\Delta F((0, 0, 1), (1, 0, 0))$ with respect to t . In the

case of Fe this approach produces an estimate of λ_{001} greater than that found experimentally.[17,18] Rather than to estimate $C_{11}-C_{12}$ from such total energy calculations, here we assume that it is relatively insensitive to composition and we follow the trends of the magnetostriction from our relativistic electronic structure calculations of B_1 .

4 The magnetic anisotropy and magnetostriction of the prototypical binary $\text{Ni}_{0.8}\text{Fe}_{0.2}$ alloy

As the first step, one-electron potentials for the fcc $\text{Ni}_{0.8}\text{Fe}_{0.2}$ and $\text{Ni}_{0.75}\text{Fe}_{0.25}$ randomly disordered bulk alloys were calculated self-consistently, using the scalar relativistic SP-KKR-CPA technique [7,8] and the atomic sphere approximation (ASA). The unit-cell volume was fixed at the experimental volume of each concentration. Exchange and correlation were accounted for using the local spin density approximation (LDA). The average spin magnetic moment of $\text{Ni}_{1-c}\text{Fe}_c$ alloy decreases slightly with decreasing Fe concentration from $1.14\mu_B$ at $c=0.25$ to the value of $1.05\mu_B$ at $c=0.2$. As c_{Fe} decreases between $0.25 > c > 0.2$, the Fe spin magnetic moment increases from $2.61\mu_B$ to $2.63\mu_B$ whereas the Ni spin moment of $0.65\mu_B$ is unchanged. These results are in good agreement with both neutron diffraction experiments and previous *ab initio* calculations. [19,20]

In Fig. 1, we plot the total, spin- and component-resolved densities of states (DOS) of $\text{Ni}_{0.8}\text{Fe}_{0.2}$ together with the band-filling curve Z_v . These also concur with previous calculations. [19,20] In common with other late transition metal strong ferromagnets, the majority spin d-states are completely filled and the majority spin DOS associated with the Fe and Ni sites are very similar displaying no evidence of the compositional disorder. This is contrary to the minority spin DOS where some of the Fe-related d-states are split away above the Ni-related ones.

Using the fully relativistic SPR-KKR-CPA method [7] we calculated the MAE of $\text{Ni}_{0.8}\text{Fe}_{0.2}$ and $\text{Ni}_{0.75}\text{Fe}_{0.25}$ and their dependence on volume conserving tetragonal distortions to obtain B_1 . The results are plotted in the upper panel of Fig. 2 together with the experimental MAE value ($2.7 \mu\text{eV}$) of bulk fcc Ni. For $c/a = 1$, $t_{[0,0,1]} = 0$, the easy axes are directed along (111) and the magnitude of the MAE ($\Delta F((001), (111))$) drops from $1.9 \mu\text{eV}$ to $0.9 \mu\text{eV}$ as c_{Fe} decreases between $0.25 < c < 0.2$. This sharp decrease in the MAE for $c \approx 0.2$ is consistent with experiment. The t -distortions, which break the cubic symmetry making the [001] and [100] directions non-equivalent, increase the MAE significantly. In Fig. 2, we plot the MAE of $\text{Ni}_{1-c}\text{Fe}_c$ as the c/a ratio is altered. The slopes of these graphs around $t = 0$ or $c/a = 1$ produce the coefficient B_1 related to the magnetostriction. The two concentrations c_{Fe} were chosen to il-

illustrate the sensitivity of MAE to the Fe content and t -deformations. B_1 is negative for both $\text{Ni}_{0.8}\text{Fe}_{0.2}$ and $\text{Ni}_{0.75}\text{Fe}_{0.25}$ and $|B_1(c_{Fe} = 0.2)| < |B_1(c_{Fe} = 0.25)|$ which is consistent with experimental observation that the magnetostriction λ passes through zero near this composition region.

In the next section we look at the effect of adding non-magnetic impurities, Cu and Mo, to nickel-iron alloys in the permalloy composition range. Experimental data suggest that both the MAE and magnetostriction are very sensitive to low concentrations of dopants. We see whether this feature is evident from the electronic structure-based calculations of the MAE and B_1 .

5 Magnetic softening in the Ni-Fe-Cu and Ni-Fe-Mo permalloys.

Properties of non-magnetic d -metals, dissolved substitutionally in ferromagnetic hosts, have been well-documented.[21,22] If a late transition metal such as Cu is added to permalloy, alongside the reduction in the amount of iron, a net decrease in the number of minority spin d -electrons is to be expected. The d -states associated with Cu will hybridise strongly with the nickel-related d -states and the Fermi energy for the alloy will be shifted upwards. There is also a net reduction in the number of minority spin d -electrons if an early transition metal such as Mo is added. The impurities will produce virtual bound states above the ferromagnetic host's majority spin d -bands and the impurity d -levels will hybridise with the host sp -conduction electrons. There will be a further hybridisation with the minority-spin d -electrons in permalloy associated with the Fe sites and an anti-parallel moment is expected on the Mo impurity sites. Pushing majority spin states above the Fermi energy by adding Mo thus enables more minority spin states to be occupied, N_\downarrow . If the MAE and magnetostriction vary with N_\downarrow , as suggested by James *et al.* [9], Cu and Mo additions to permalloy should have similar effects on these quantities. Our results broadly bear this out. The spin magnetic moments, number of valence electrons and number of minority spin electrons calculated for various ternary Ni-Fe-Cu and Ni-Fe-Mo alloys are given in Table.1.

In Fig. 2 we display $\Delta F((001), (111))$, $\Delta F((001), (110))$ and $\Delta F((001), (111))$ of 5 at.% Cu(Mo) Ni-Fe-Cu(Mo) alloys, as the c/a ratio is altered. The trends in the MAE and B_1 for both the Cu- and Mo-doped alloys are roughly similar but there are some differences. In the case of Ni-Fe-Cu, (i) the easy axis is along $[111]$ while the magnitude of MAE never exceeds $1 \mu\text{eV}$ at $c/a = 1$, and (ii) the B_1 gradually decreases with increasing c_{Fe} to a near zero value at $c_{Fe} = 0.225$. For the Ni-Fe-Mo system, (i) the easy axis along $[100]$ is perpendicular to the magnetisation direction, (ii) the MAE values are nearly zero, and (iii) B_1 changes the sign when c_{Fe} varies between 0.2 and 0.225. In both cases impurity-doping changes the magnetic anisotropy and magnetostriction of Ni-

rich Ni-Fe in such a way that enhances their permeability.

The differences in the total DOS when c/a varies, ΔDOS , of $\text{Ni}_{0.75}\text{Fe}_{0.2}\text{Cu}_{0.05}$ and $\text{Ni}_{0.75}\text{Fe}_{0.2}\text{Mo}_{0.05}$ between the magnetization directions along $[001]$ and $[111]$ are plotted in Fig. 3. The comparison with the corresponding ΔDOS s of binary $\text{Ni}_{0.8}\text{Fe}_{0.2}$ illustrates the doping effect on the magnetic softening. We note from Fig. 2 that changing the composition of permalloy from $\text{Ni}_{0.80}\text{Fe}_{0.20}$ to $\text{Ni}_{0.80}\text{Fe}_{0.15}\text{Cu}_{0.05}$ or $\text{Ni}_{0.80}\text{Fe}_{0.15}\text{Mo}_{0.05}$ has switched the sign of the slope, B_1 , of these lines. This suggests that at some intermediate doping level, B_1 and therefore the magnetostriction should be zero. Before embarking on a course of further calculations for ternary alloys in this composition region we tested a model based upon the parent $\text{Ni}_{0.80}\text{Fe}_{0.20}$ system.

Fig. 4 shows all three magnetic anisotropy energies, $\Delta F((001), (111))$, $\Delta F((001), (110))$ and $\Delta F((001), (111))$ for $\text{Ni}_{0.80}\text{Fe}_{0.20}$ as a function of the tetragonal distortion t . B_1 from all three curves is negative. We also see how the MAE and B_1 changes when the Fermi energy is shifted upwards to mimic roughly the effect of alloying with non-magnetic dopants by increasing the number of minority spin-electrons. With the ‘correct’ band-filling (Fermi energy unshifted) ($Z_v=9.6$ el.), the sign of B_1 is negative as shown also in Fig. 2. When $Z_v=9.85$ el. (corresponding to $E_F+0.14$ eV) the MAE is tiny and the slope $B_1 \sim 0$ implying a very small magnetostriction ($\lambda \simeq 0$). Further increase of E_F causes B_1 to become larger and positive, increasing the magnitude of λ . We now see if we can reproduce this situation by doping with a non-magnetic transition metal.

Fixing the Ni concentration at $c_{\text{Ni}}=0.8$ we calculated the MAE and B_1 over a narrow range of Cu concentration, $3 < c_{\text{Cu}} < 5$ at.%. Fig. 5 shows the results. In line with the scenario described in Fig. 4, the MAE and B_1 become vanishing small when between 3 and 4 % of Cu is added. The ternary alloys $\text{Ni}_{0.80}\text{Fe}_{0.17-\delta}\text{Cu}_{0.03+\delta}$, $0 < \delta < 0.01$ are therefore very soft magnets, since the easy-axis direction switches and B_1 , changes sign. Hence, for this narrow composition range of Ni-Fe-Cu, the magnetostriction coefficients, $\lambda \rightarrow 0$ while the MAE value remains low enough for this alloy to develop high permeability.

From the MAE calculations of pure Fe and Ni we know that the lattice constant is also an important factor. Here we have used the experimental lattice constants and therefore, the magnetovolume effect has not been examined. Our SPR-KKR-CPA calculations have been used to study the effect of the variation of doping with an early and late transition metal on the magnetic anisotropy properties of permalloys and give an explanation of the experimentally observed and well-known facts on the preparation of the high permeability materials. In particular we have demonstrated why extremely soft magnetic properties of Ni-Fe-Cu(Mo) are developed for rather narrow concentration ranges of the Cu/Mo dopants, depending on the Fe content in Ni-rich

compositions. Up to now we have assumed that the alloys are completely compositionally disordered. Preparation procedures for high permeability permalloys, however, do instill varying degrees of long- or short-range compositional order which alter the magnetic properties significantly. We study this aspect in the next sections.

6 Compositional order and magnetic anisotropy

Ordering in alloys can be conveniently and succinctly classified in terms of static concentration waves.[23] For example, at high temperatures, a binary alloy A_cB_{1-c} where the atoms are arranged on a regular array of lattice sites, has each of its sites occupied by either an A - or B -type atom with probabilities c and $(1 - c)$ respectively. In general, in terms of a set of site-occupation variables $\{\xi_i\}$, (with $\xi_i = 1(0)$ when the i -th site in the lattice is occupied by an $A(B)$ -type atom) the thermodynamic average, $\langle \xi_i \rangle$, of the site-occupation variable is the concentration c_i at that site and for the solid solution $c_i = c$ for all sites. Below some transition temperature, T_o , the system orders or phase separates so that a compositionally modulated alloy forms. The temperature-dependent fluctuations of the concentrations about the solid solution value c , $\{\delta c_i\} = \{c_i - c\}$, can be pictured as a superposition of static concentration waves,[23,24] i.e.,

$$c_i = c + \frac{1}{2} \sum_{\mathbf{q}} \left[c_{\mathbf{q}} e^{i\mathbf{q} \cdot \mathbf{R}_i} + c_{\mathbf{q}}^* e^{-i\mathbf{q} \cdot \mathbf{R}_i} \right],$$

where, $c_{\mathbf{q}}$ are the amplitudes of the concentration waves with wave-vectors \mathbf{q} , and \mathbf{R}_i are the lattice positions. Usually only a few concentration waves are needed to describe a particular ordered structure. For example, the CuAu-like $L1_0$ tetragonal ordered structure is set up by a single concentration wave with $c_{\mathbf{q}} = \frac{1}{2}$ and $\mathbf{q} = (001)$ (\mathbf{q} is in units of $\frac{2\pi}{a}$, a being the lattice parameter). The Cu_3Au $L1_2$ ordered phase which $\text{Ni}_{0.75}\text{Fe}_{0.25}$ forms below $T = 900\text{K}$, is set by three waves with $\mathbf{q} = (001)$, (010) and (100) .

The Free Energy of a partially ordered alloy can be estimated in terms of a quantity $S_{ij}^{(2)}$

$$S_{jk}^{(2)}(\mathbf{e}) = - \left. \frac{\partial^2 \Omega(\{c_i\}; \mathbf{e})}{\partial c_j \partial c_k} \right|_{\{c_i=c\}},$$

i.e. a second derivative with respect to concentration of the Grand Potential describing the interacting electron system which constitutes the alloy. [24]

$S_{ij}^{(2)}$ is formally a direct pair correlation function but can loosely be pictured as an effective atom-atom interchange energy. It is determined by the electronic structure of the disordered phase, the solid solution. The atomic short-range order, $\alpha_{ij} = \beta[\langle \xi_i \xi_j \rangle - \langle \xi_i \rangle \langle \xi_j \rangle]$, whose lattice Fourier transform $\alpha(\mathbf{q}, T)$ can be measured by diffuse scattering experiments, is related directly via $\alpha(\mathbf{q}, T) = \beta c(1 - c)/(1 - \beta c(1 - c)S^{(2)}(\mathbf{q}))$ where $S^{(2)}(\mathbf{q})$ is the lattice Fourier transform of $S_{ij}^{(2)}$. The spinodal transition temperature T_o , below which the alloy orders into a structure characterized by the concentration wave-vector \mathbf{q}_{max} , is determined by $S^{(2)}(\mathbf{q}_{max})$, where \mathbf{q}_{max} is the value at which $S^{(2)}(\mathbf{q})$ is maximal ($\mathbf{q}_{max} = (0, 0, 1)$ for $L1_0$ order). We can write, [24,25] $T_o = c(1 - c)S^{(2)}(\mathbf{q}_{max})/k_B$. Calculations of $S^{(2)}(\mathbf{q})$ then can provide a quantitative description of the propensity of an alloy to order when thermally annealed.

The MAE of a ferromagnetic alloy with a compositional modulation can be defined in terms of the difference between the free energies of the system magnetised along two different directions \mathbf{e}_1 and \mathbf{e}_2 . If the modulation is specified by a concentration wave of amplitude $c_{\mathbf{q}}$ and wavevector \mathbf{q} , this difference can be approximately written as

$$\Delta F(\mathbf{e}_1, \mathbf{e}_2) \approx \Delta F^{dis.}(\mathbf{e}_1, \mathbf{e}_2) - K(\mathbf{q}; \mathbf{e}_1, \mathbf{e}_2)|c_{\mathbf{q}}|^2 \quad (7)$$

where $K(\mathbf{q}; \mathbf{e}_1, \mathbf{e}_2) = \frac{1}{2}[S^{(2)}(\mathbf{q}; \mathbf{e}_1) - S^{(2)}(\mathbf{q}; \mathbf{e}_2)]$, half the difference between the direct correlation function $S^{(2)}(\mathbf{q})$ for the ferromagnetic alloy magnetised along \mathbf{e}_1 and along \mathbf{e}_2 . $\Delta F^{dis.}$ is the MAE of the completely disordered alloy [7] which we have calculated earlier in this paper for Ni-Fe, Ni-Fe-Cu and Ni-Fe-Mo. For an alloy with atomic short range order $\alpha(\mathbf{q}; T)$ the MAE is expressed

$$\Delta F(\mathbf{e}_1, \mathbf{e}_2) \approx \Delta F^{dis.}(\mathbf{e}_1, \mathbf{e}_2) - \frac{1}{V_{BZ}} k_B T \int d\mathbf{q}' K(\mathbf{q}'; \mathbf{e}_1, \mathbf{e}_2) \alpha(\mathbf{q}', T; \mathbf{e}_1) \quad (8)$$

Now $\alpha(\mathbf{q}, T; \mathbf{e}_1)$ is a structured function of \mathbf{q} with peaks located at \mathbf{q}_{max} , wavevectors of the concentration waves which characterise the ordered phase the alloy can form at low temperatures at equilibrium. Just above T_o where the ASRO is pronounced the second term becomes $\approx -c(1 - c)K(\mathbf{q}_{max}; \mathbf{e}_1, \mathbf{e}_2)$. Full details on how the dependence of MAE on compositional ordering can be calculated from ab-initio electronic structure calculations can be found in references [7,8]. Another aspect of this approach can be obtained from calculating $S^{(2)}(\mathbf{q}; \mathbf{e})$ for different \mathbf{q} -vectors, whilst keeping the magnetic field and magnetization direction fixed and gives a quantitative description of the phenomenon of magnetic annealing [8] in which an applied magnetic field can cause directional compositional ordering. For a magnetically soft alloy such as the 75 % Ni permalloy this leads to a significant uniaxial anisotropy.[7] In addition to permalloy, we have also used this approach to investigate the relation

of MAE to compositional order in $\text{Fe}_{0.5}\text{Co}_{0.5}$, $\text{Co}_{0.5}\text{Pt}_{0.5}$ and $\text{Fe}_{0.5}\text{Pd}_{0.5}$. [26]

In the next section we use this approach to investigate how the effect of compositional order on the magnetic anisotropy of permalloy $\text{Ni}_{0.80}\text{Fe}_{0.20}$ varies as the number of minority spin electrons is increased. Once again this can be taken as a simple model of the influence of adding non-magnetic impurities.

7 The dependence of the magnetocrystalline anisotropy of $\text{Ni}_{0.8}\text{Fe}_{0.2}$ upon chemical order

As expected from its inherent cubic symmetry and confirmed by our calculations, completely disordered fcc- $\text{Ni}_{0.8}\text{Fe}_{0.2}$ has a tiny magnetic anisotropy ($\Delta F^{dis.}((0, 0, 1), (1, 1, 1)) < 1\mu\text{eV}$). This is demonstrated in the upper panel of Fig. 6 and discussed earlier. The magnetic anisotropy is further reduced by shifting the Fermi energy upwards so that N_{\downarrow} is increased. The lower panel of Fig. 6 shows what happens to $K(\mathbf{q}'; (001), (100))$ and $K(\mathbf{q}'; (001), (111))$ for similar circumstances. For the ‘correct’ E_F , ($Z_{\nu} = 9.6$ electrons), the values suggest a significant enhancement of the magnetic anisotropy if there is directional long- or short-range order in $\text{Ni}_{0.8}\text{Fe}_{0.2}$. As E_F is shifted upwards so that $Z_{\nu} = 9.7$, $K(\mathbf{q}'; (001), (100))$ and $K(\mathbf{q}'; (001), (111))$ double in size but then drop sharply to zero when the band-filling reaches 9.83. The MAE and B_1 of the disordered alloy are also very small at this band-filling. We can deduce therefore that a ternary alloy with composition near $\text{Ni}_{0.80}\text{Fe}_{0.17}\text{Cu}_{0.03}$, compatible with this band-filling, may have high permeability which is also rather insensitive to its preparation conditions. Fig. 6, moreover, shows that this insensitivity is expected only for a very narrow composition range.

8 Summary

Calculations of the magnetic anisotropy and the trends for magnetostriction in fcc 80 % Ni based Ni-Fe permalloys have been carried out, using the fully relativistic spin-polarized KKR method within the CPA. The reliability of this method to model magnetic anisotropy in soft magnetic materials has been demonstrated. The trends found in the MAE calculations for $\text{Ni}_{0.8}\text{Fe}_{0.2}$ are in a good agreement with those found in experiments. A description of magnetic softening caused by doping with non-magnetic metals Cu and Mo has been given. We have linked these results to further calculations for $\text{Ni}_{0.8}\text{Fe}_{0.2}$ where the number of minority-spin electrons has been artificially increased. Our estimates of the effects of atomic short- and long-range chemical order on the magnetic anisotropy of these permalloys show strong variation with composition. Pooling the results, we have managed to follow the well-known

empirical trends and to show how a potentially perfect permalloy might be found with zero magnetic anisotropy and zero magnetostriction and which is also rather insensitive to its preparation conditions.

9 Acknowledgments

We acknowledge support from the EPSRC (UK) and computing resources at the Centre for Scientific Computing, University of Warwick.

References

- [1] E. du Tremolét de Lacheisserie, *Magnetostriction: Theory and Applications of Magnetoelasticity* (CRC Press, Boca Raton, 1993).
- [2] S.Chikazumi, *Physics of Ferromagnetism*, (Oxford Science Publications, 1999).
- [3] T.Wakiyama, *Physics and Engineering Applications of Magnetism*, ed. Y.Ishikawa and N.Miura, Springer Series in Solid State Sciences **92**, 133, (1991).
- [4] F.Pfeifer and C.Radeloff, J. Magn. Magn. Mater. **19**, 190 (1980).
- [5] H.H.Scholefield, R.V.Major, B.Gibson and A.P.Martin, Brit.J.Appl.Phys. **18**, 41, (1967).
- [6] S.Ostanin, J.B.Staunton, S.S.A.Razee, C. Demangeat, B. Ginatempo and Ezio Bruno, Phys. Rev. B **69**, 064425 (2004).
- [7] S.S.A.Razee, J.B.Staunton, and F.J.Pinski, Phys. Rev. B **56**, 8082 (1997).
- [8] S.S.A.Razee, J.B.Staunton, B.Ginatempo, F.J.Pinski, and E. Bruno, Phys. Rev. Lett. **82**, 5369 (1999).
- [9] P.James, O.Eriksson, O.Hjortstam, B.Johansson, L.Nordstrom, Appl. Phys. Lett. **76**, 915, (2000).
- [10] H.J.F.Jansen, Phys. Rev. B **59**, 4699 (1999).
- [11] A.R.Mackintosh and O.K.Andersen, in *Electrons at the Fermi Surface*, edited by M.Springfold (Cambridge University Press, Cambridge, 1980); M.Weinert, R.E.Watson, and J.W.Davenport, Phys. Rev. B **32**, 2115 (1985).
- [12] P.Lloyd and P.V.Smith, Adv.Phys. **21**, 69, (1972).
- [13] B.Ginatempo and E.Bruno, Phys.Rev.B **55**, 12946, (1997).
- [14] R.C.O’Handley, *Modern Magnetic Materials Principles and Applications* (Wiley, 2000).

- [15] O.Hjortstam, K.Baberschke, J.M.Wills, B.Johansson, and O.Eriksson, Phys. Rev. B **55**, 15026 (1997).
- [16] L.Fast, J.M.Wills, B.Johansson, and O.Eriksson, Phys. Rev. B **51**, 17431 (1995).
- [17] A.J.Freeman, R.Q.Wu, M.Y.Kim, and V.I.Gavrilenko, J. Magn. Magn. Mater. **203**, 1 (1999).
- [18] R.Wu and A.J.Freeman, J. Appl. Phys. **79**, 6209 (1996).
- [19] D.D.Johnson, F.J.Pinski, and J.B.Staunton, J. Appl. Phys. **61**, 3715 (1987).
- [20] J.B.Staunton, D.D.Johnson and B.L.Gyorffy, J. Appl. Phys. **61**, 3693 (1987).
- [21] D.G.Pettifor, *Bonding and Structure of Molecules and Solids* (Oxford University Press, 1995).
- [22] P.H.Dederichs *et al.*, J.Mag.Magn.Mat. **100**, 1-3,241-260, (1991); R.Zeller, J.Phys.F **17**, 2123, (1987).
- [23] A.G.Khachaturyan, *Theory of Structural Transformations in Solids* (Wiley, N.Y., 1983), p.39.
- [24] B.L.Gyorffy and G.M.Stocks, Phys. Rev. Lett. **50**, 374 (1983).
- [25] J.B.Staunton, D.D.Johnson and F.J.Pinski, Phys. Rev. B **50**, 1450 (1994).
- [26] S.S.A.Razee, J.B. Staunton, B. Ginatempo, E. Bruno, and F.J. Pinski, Phys. Rev. B **64**, 014411 (2001).

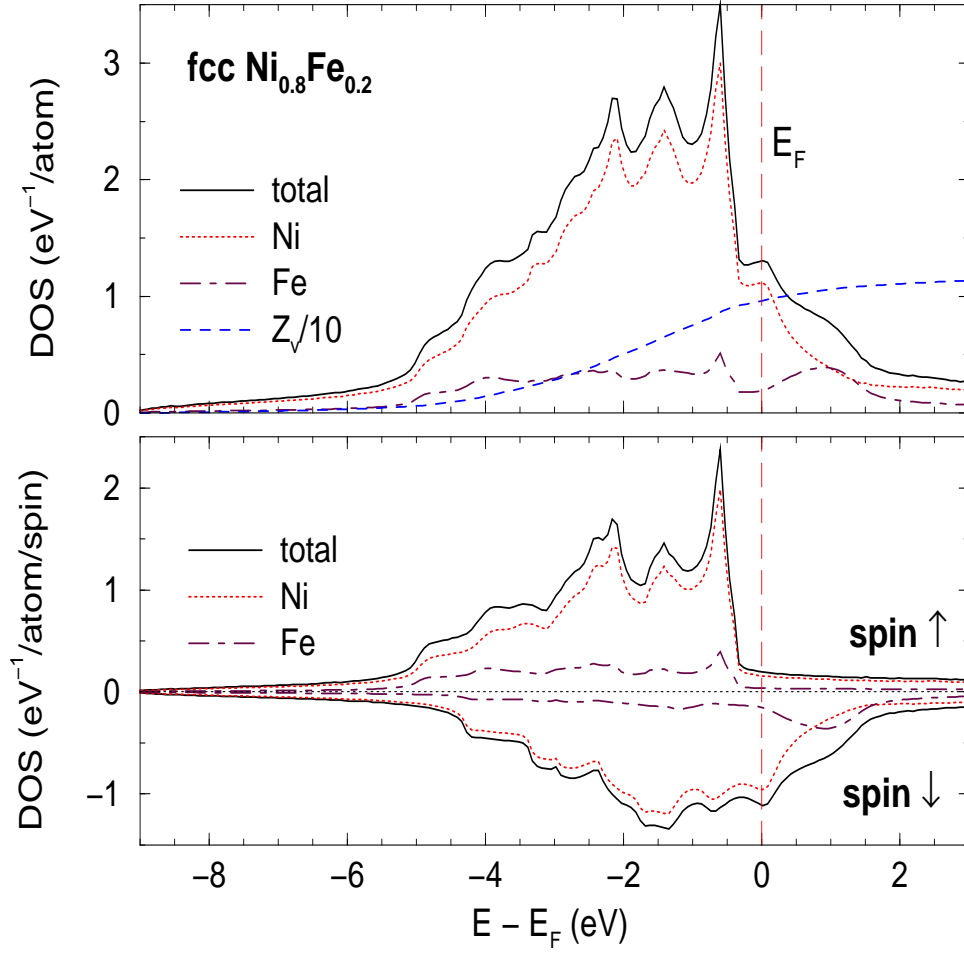


Fig. 1. The component-resolved and total DOS of $\text{Ni}_{0.8}\text{Fe}_{0.2}$ are shown in the upper panel (a) together with the band-filling curve Z_v . In the (b) panel, the spin-projected DOS are shown.

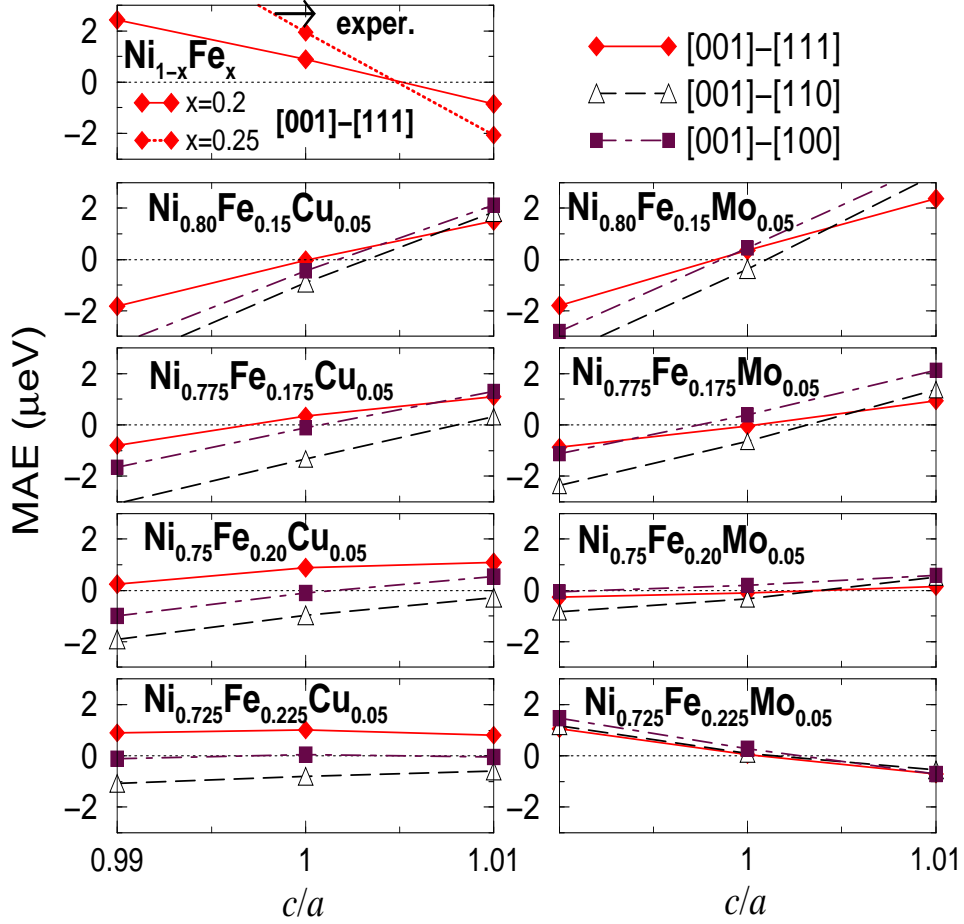


Fig. 2. The MAE, $\Delta F((001), \mathbf{e}_2)$, with $\mathbf{e}_2 = (100)$, (110) and (111) of randomly disordered fct $\text{Ni}_{1-c}\text{Fe}_c$, calculated by SPR-KKR-CPA, is shown as a function of tetragonal c/a variations in the upper (left) panel. The experimental MAE value of bulk fcc Ni is marked by an arrow. In the following four left (right) panels, we plot the variations of ΔF 's with respect to c/a for the ternary Ni-Fe-Cu(Mo) alloys doped with 5 at.% Cu (Mo).

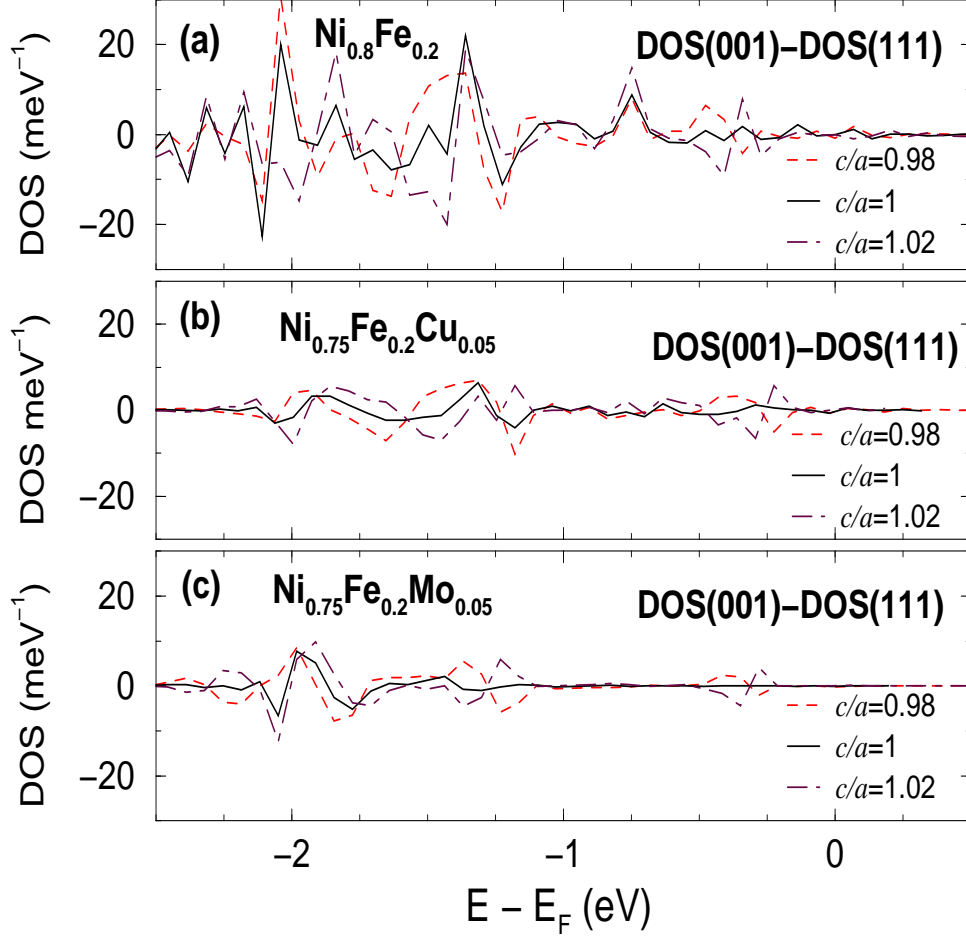


Fig. 3. The differences in the total DOS of Ni_{0.8}Fe_{0.2} between the magnetization directions along [001] and [111] are plotted in panel (a) for perfect cubic structure, the tetragonal compression ($c/a = 0.98$) and elongation ($c/a = 1.02$). The corresponding Δ DOS of Ni_{0.75}Fe_{0.2}Cu_{0.05} and Ni_{0.75}Fe_{0.2}Mo_{0.05} are shown in the (b) and (c) panels, respectively.

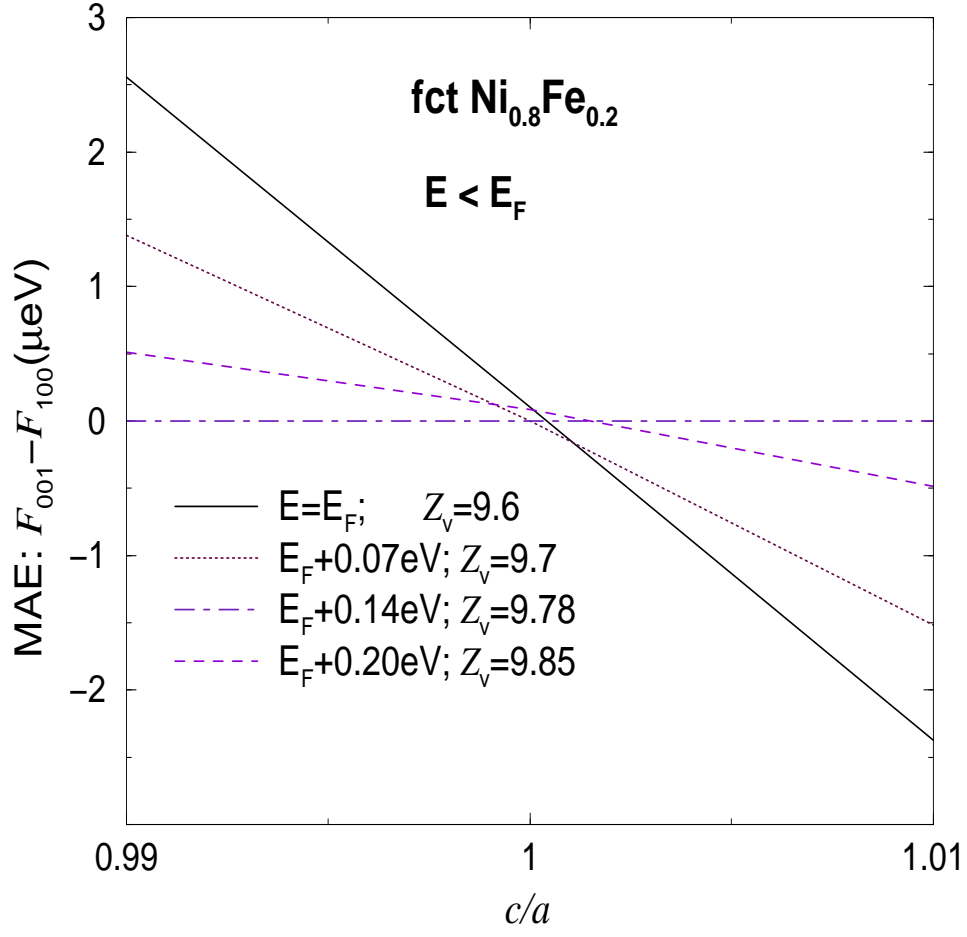


Fig. 4. The MAE, $\Delta F((001), (100))$, of $\text{Ni}_{0.8}\text{Fe}_{0.2}$ as a function of the t -deformations for several different band-fillings.

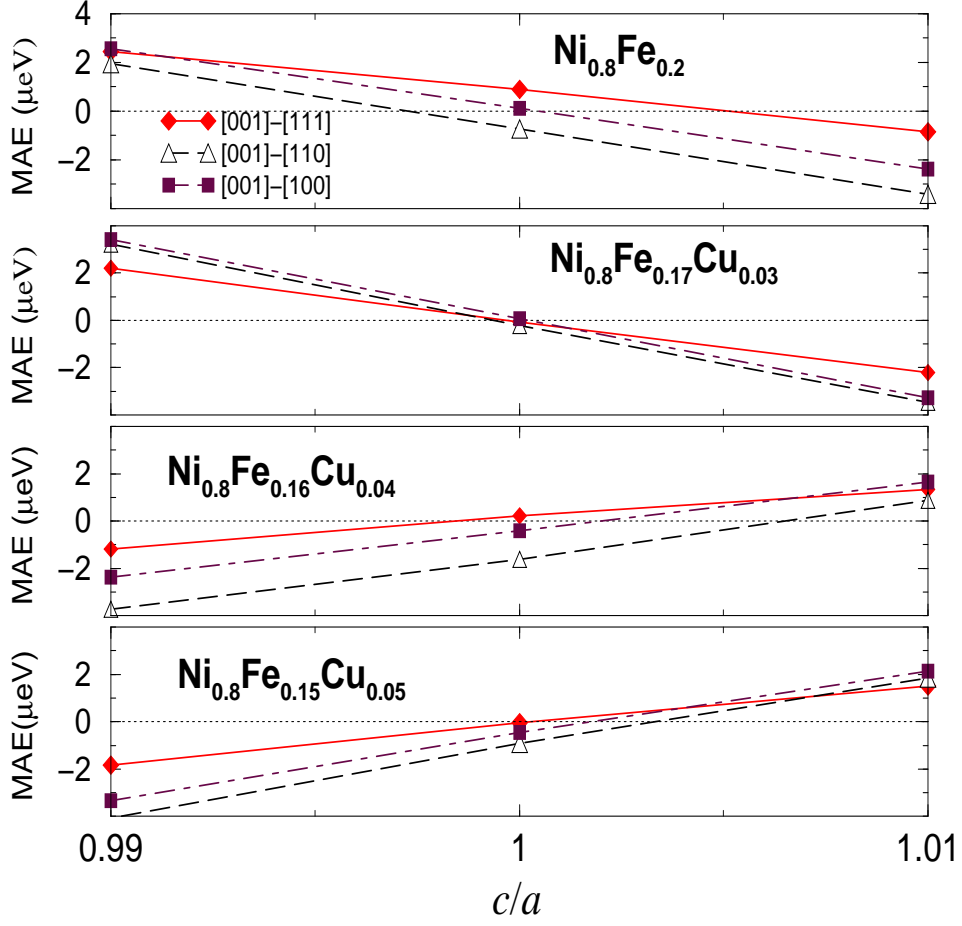


Fig. 5. The MAE $\Delta F((001), \mathbf{e}_2)$ for $\mathbf{e}_2 = (111)$, (110) and (100) as a function of tetragonal deformations for the 80 % Ni based permalloys. The ΔF 's of the $\text{Ni}_{0.8}\text{Fe}_{0.2}$ binary alloy are plotted in the upper panel. In the three lower panels, we show how the sign of the slope, B_1 , is changed when concentration of dopant (Cu) varies between 3 and 5 at.%.

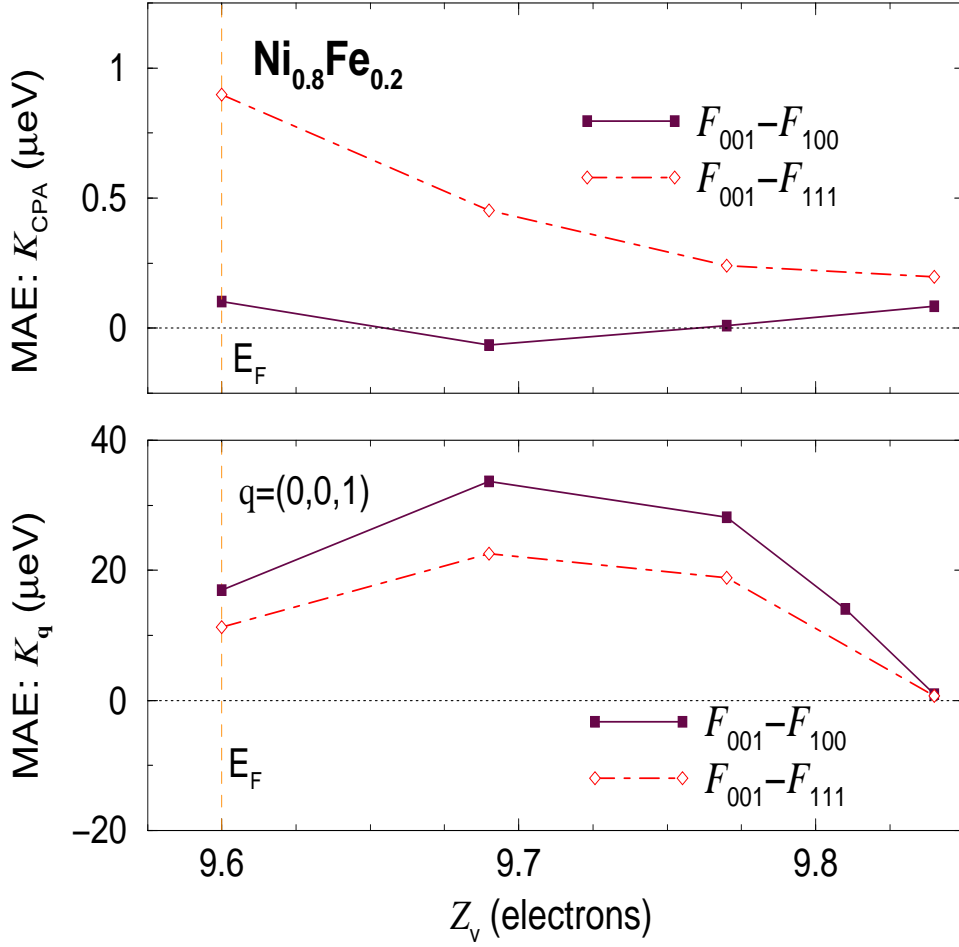


Fig. 6. The $\Delta F((001), \mathbf{e}_2)$'s for $\mathbf{e}_2 = (100)$ and (111) of the randomly disordered $\text{Ni}_{0.8}\text{Fe}_{0.2}$ alloy are shown in the upper panel as a function of the band-filling parameter Z_v . In the lower panel, the corresponding variation of the ΔF 's with composition modulation, i.e. $K(\mathbf{q}; (001), \mathbf{e}_2)$ calculated for the modulation $\mathbf{q} = (0, 0, 1)$ are plotted as functions of Z_v .

	μ^{Ni}	μ^{Fe}	$\mu^{Cu(Mo)}$	$\bar{\mu}$	Z_ν	N_\downarrow
Ni _{0.725} Fe _{0.225} Cu _{0.05}	0.58	2.59	0.06	1.01	9.60	8.59
Ni _{0.725} Fe _{0.225} Mo _{0.05}	0.39	2.30	-0.12	0.79	9.35	8.56
Ni _{0.75} Fe _{0.25}	0.65	2.61	—	1.14	9.50	8.36
Ni _{0.75} Fe _{0.2} Cu _{0.05}	0.57	2.63	0.05	0.96	9.65	8.69
Ni _{0.75} Fe _{0.2} Mo _{0.05}	0.42	2.37	-0.08	0.79	9.40	8.61
Ni _{0.775} Fe _{0.175} Cu _{0.05}	0.58	2.62	0.05	0.91	9.70	8.79
Ni _{0.775} Fe _{0.175} Mo _{0.05}	0.41	2.39	-0.08	0.73	9.45	8.72
Ni _{0.8} Fe _{0.2}	0.65	2.63	—	1.05	9.60	8.55
Ni _{0.8} Fe _{0.15} Cu _{0.05}	0.58	2.66	0.04	0.87	9.75	8.88
Ni _{0.8} Fe _{0.15} Mo _{0.05}	0.40	2.40	-0.07	0.68	9.50	8.82

Table 1

The component-resolved μ^α , average spin magnetic moments $\bar{\mu}$ (in μ_B), band-filling Z_ν and minority spin electrons $N_\downarrow = Z_\nu - \bar{\mu}$ in 80 % based Ni permalloys.